A Letters Journal Exploring the Frontiers of Physics

AN INVITATION TO SUBMIT YOUR WORK

www.epljournal.org

The Editorial Board invites you to submit your letters to EPL

EPL is a leading international journal publishing original, innovative Letters in all areas of physics, ranging from condensed matter topics and interdisciplinary research to astrophysics, geophysics, plasma and fusion sciences, including those with application potential.

The high profile of the journal combined with the excellent scientific quality of the articles ensures that EPL is an essential resource for its worldwide audience. EPL offers authors global visibility and a great opportunity to share their work with others across the whole of the physics community.

Run by active scientists, for scientists

EPL is reviewed by scientists for scientists, to serve and support the international scientific community. The Editorial Board is a team of active research scientists with an expert understanding of the needs of both authors and researchers.

OVER
560,000
full text downloads in 2013

24 DAYS
average accept to online publication in 2013

10,755
citations in 2013

"We greatly appreciate the efficient, professional and rapid processing of our paper by your team."

Cong Lin
Shanghai University

Six good reasons to publish with EPL

We want to work with you to gain recognition for your research through worldwide visibility and high citations. As an EPL author, you will benefit from:

1. **Quality** – The 50+ Co-editors, who are experts in their field, oversee the entire peer-review process, from selection of the referees to making all final acceptance decisions.
2. **Convenience** – Easy to access compilations of recent articles in specific narrow fields available on the website.
3. **Speed of processing** – We aim to provide you with a quick and efficient service; the median time from submission to online publication is under 100 days.
4. **High visibility** – Strong promotion and visibility through material available at over 300 events annually, distributed via e-mail, and targeted mailshot newsletters.
5. **International reach** – Over 2600 institutions have access to EPL, enabling your work to be read by your peers in 90 countries.
6. **Open access** – Articles are offered open access for a one-off author payment; green open access on all others with a 12-month embargo.

Details on preparing, submitting and tracking the progress of your manuscript from submission to acceptance are available on the EPL submission website **www.epletters.net**.

If you would like further information about our author service or EPL in general, please visit **www.epljournal.org** or e-mail us at **info@epljournal.org**.

EPL is published in partnership with:

European Physical Society | Società Italiana di Fisica | EDP Sciences | IOP Publishing

A Letters Journal Exploring the Frontiers of Physics

September 2015

EPL, **111** (2015) 68007
doi: 10.1209/0295-5075/111/68007

www.epljournal.org

Extreme brain events: Higher-order statistics of brain resting activity and its relation with structural connectivity

T. A. Amor[1(a)], R. Russo[2(a)], I. Diez[3], P. Bharath[4], M. Zirovich[4], S. Stramaglia[5,6], J. M. Cortes[3,7,8], L. de Arcangelis[9(b)] and D. R. Chialvo[10]

[1] *Physics Department, Faculty of Exact and Natural Sciences, University of Buenos Aires Buenos Aires, Argentina*
[2] *Physics Department, University of Naples Federico II - Napoli, Italy*
[3] *Biocruces Health Research Institute, Cruces University Hospital - Barakaldo, Spain*
[4] *VA West Los Angeles Medical Center - Los Angeles, CA, USA*
[5] *Dipartimento di Fisica, Università di Bari and INFN Sezione di Bari - Bari, Italy*
[6] *BCAM - Basque Center for Applied Mathematics - Bilbao, Spain*
[7] *Ikerbasque, The Basque Foundation for Science - Bilbao, Spain*
[8] *Department of Cell Biology and Histology. University of the Basque Country - Leioa, Spain*
[9] *Department of Industrial and Information Engineering, Second University of Naples and INFN Gr. Coll. Salerno - Aversa (CE), Italy*
[10] *National Scientific and Technical Research Council (CONICET) - Buenos Aires, Argentina*

received 7 May 2015; accepted in final form 15 September 2015
published online 7 October 2015

PACS 89.75.Fb – Structures and organization in complex systems
PACS 05.45.Tp – Time series analysis
PACS 87.19.lf – MRI: anatomic, functional, spectral, diffusion

Abstract – The brain exhibits a wide variety of spatiotemporal patterns of neuronal activity recorded using functional magnetic resonance imaging as the so-called blood-oxygenated-level–dependent (BOLD) signal. An active area of work includes efforts to best describe the plethora of these patterns evolving continuously in the brain. Here we explore the third-moment statistics of the brain BOLD signals in the resting state as a proxy to capture extreme BOLD events. We find that the brain signal exhibits typically nonzero skewness, with positive values for cortical regions and negative values for subcortical regions. Furthermore, the combined analysis of structural and functional connectivity demonstrates that relatively more connected regions exhibit activity with high negative skewness. Overall, these results highlight the relevance of recent results emphasizing that the spatiotemporal location of the relatively large-amplitude events in the BOLD time series contains relevant information to reproduce a number of features of the brain dynamics during resting state in health and disease.

Introduction. – The brain behavioral and cognitive repertoire is directly related to its ability to sustain a wide variety of spatiotemporal patterns of neuronal activity. The recent advent of a diversity of neuro-imaging techniques allows for the direct observation of these patterns and the design of experiments to relate dynamics with cognition and behavior. At the same pace, in functional magnetic resonance imaging (fMRI) the size of the datasets of the brain signal (the so-called blood-oxygenated-level–dependent or BOLD signal) is such that novel numerical techniques are needed for a more efficient signal representation and processing.

Following the initial studies on complex-network analysis of fMRI [1,2] we have witnessed important advances in the last decade by a plethora of studies uncovering the details of complex networks underlying both brain structure and function at the macroscale [3–5]. The brain neural dynamics and its associated functions are constrained by the underlying wiring structure [6,7], (*i.e.*, the so-called structural connectivity, SC). A fundamental problem in neuroscience is to understand how the same fixed structure

(a) Both authors contributed equally to this work.
(b) E-mail: lucilla.dearcangelis@unina2.it (corresponding author)

gives rise to the large repertoire of functional correlations (sometimes called functional connectivity, FC). This is relevant because these correlations are reflecting the transient states which are associated with perception, cognition and action. This issue has been studied starting by the earlier studies of Sporns [8,9] followed by others using combined structure-function datasets [10–16].

At the same time, but from a different perspective, recent results emphasize that the space-time location of the relatively large amplitude events in the BOLD time series contains enough information to reproduce a number of features describing the brain dynamics in the resting state [17–20]. In the same direction, the presence of correlations between relatively brief but large events in brain activity is already documented [21]. The present work investigates further details of their statistics and the relation of their features with the properties of the underlying structural connectivity network.

The paper is organized as follows: In the next section the two datasets analyzed are described: The first one corresponds to fMRI recordings used to establish the higher-order statistics of the resting state, whereas the second one allows to investigate these features in relation to the underlying structural connectivity. Results first report on the distribution and spatial localization of extremal events, leading to a peculiar distribution of skewness across brain structures. The results are compared with a recent description of asymmetry in the variance, which is shown to be simply proportional to the skewness. Moreover, a potentially important source of spurious artifacts is rejected showing that the observed higher-order statistics are unrelated to head motion during the recordings. Finally a combined structural and functional statistical analysis is made to demonstrate the presence of correlations among extreme events in brain activity and node connectivity. A final discussion will stress the relevance of these results to brain function.

Methods. – Two different datasets were analyzed in this work, one for the study of the higher-order statistics and a second one for the combined structure-dynamics analysis. The first database corresponds to data obtained at the University of California, Los Angeles (UCLA), performed with a SIEMENS Magnetom TrioTim Syngo MR B15 scanner, we will call it the UCLA cohort. The second dataset corresponds to data obtained in Cruces University Hospital (Bilbao, Spain) using a Philips Achieva 1.5 T Nova scanner, here referred as the Bilbao cohort.

Bilbao cohort. This dataset comprises recordings of structural and functional imaging in 12 (6 males) healthy subjects, aged between 24 and 46 (33.5 ± 8.7) who provided information consent forms before the imaging session. This work was approved by the Ethics Committee at the Cruces University Hospital; High-resolution anatomical MRI was acquired using a T1-weighted 3D sequence (TR = 7.482 ms, TE = 3.425 ms; parallel imaging (SENSE) acceleration factor = 1.5; acquisition matrix size = 256×256; FOV = 26 cm; slice thickness = 1.1 mm; 170 contiguous sections). Diffusion weighted images (DWIs) were acquired using pulsed gradient-spin-echo echo-planar-imaging (PGSE-EPI) (TR = 11070.28 ms, TE = 107.04 ms; 60 slices with thickness of 2 mm; no gap between slices; 128×128 matrix with an FOV of 23×23 cm). Changes in blood-oxygenation-level–dependent (BOLD) T2* signals were measured using an interleaved gradient-echo EPI sequence. The subjects lay quietly for 7.28 minutes, and 200 whole brain volumes were obtained (TR = 2.200 ms, TE = 35 ms; flip angle 90; 24 cm field of view; 128×128 pixel matrix; and $3.12 \times 3.19 \times 4.00$ mm voxel dimensions).

Structural data preprocessing: To analyze the diffusion weighted images we first applied the eddy current correction to overcome artifacts produced by changes in the gradient field directions of the MR scanner and subject's head movement. Then, a local fitting of the diffusion tensor was applied to compute the diffusion tensor model at each voxel. Subsequently, a FACT (fiber assignment by continuous tracking) deterministic tractography algorithm [22] was employed, by using interactive software for fiber tracking called "Diffusion Toolkit" [23]. Tractography algorithms were developed to reconstruct white-matter pathways in the brain connecting grey-matter regions from diffusion tensor imaging (DTI) data. The FACT algorithm reconstructs individual fibers and tracks them by connecting the voxel where the fiber is initiated with the adjacent one towards the fiber direction, and by iterating this procedure until it is terminated according to the criterion that the fiber arrives to a grey matter region. To avoid sharp curvatures of axonal tracts we fixed a maximum angle variation of 35 degrees from a given voxel to the following one (see [24]).

To calculate the structural connectivity matrices we computed the transformation from MNI152 brain template to individual fractional anisotropy maps. Using this transformation, the 2514 region atlas was transformed to the diffusion image space. Finally, the structural connectivity matrices were obtained by counting the number of fibers connecting each individual pair of ROIs.

Functional data preprocessing: The fMRI data was preprocessed using FMRIB Expert Analysis Tool (FEAT [25], `www.fmrib.ox.ac.uk/fsl`). The first 10 volumes were discarded to avoid saturation effects, and the remaining volumes were corrected for motion and slice timing. Spatial smoothing was done with a 6 mm FWHM isotropic Gaussian kernel and a band pass filter was applied between 0.01 and 0.08 Hz [26]. Using MCFLIRT, motion time courses, average cerebrospinal fluid (CSF) signal, average white-matter signal and average global signal were regressed out. Despiking and testing for additional scanner artifacts were done using tools from FSL. Finally, the functional data were spatially normalized to the MNI152 brain template to a resolution of $3 \times 3 \times 3$ mm.

ROI extraction: We applied the method of spatially constrained clustering to functional data averaged over the

subjects ($n = 12$) in order to extract the regions of interest (ROIs), as explained in [27], and allow for the generation of common ROIs. A spatial constraint is imposed to ensure that the resulting ROIs are spatially coherent and clustering was performed based on temporal correlations between voxel time series. To cluster at the group level, a 2-level approach was applied in which the single-subject data were first clustered and then all the subjects data were combined to perform a second clustering. Finally, we applied a parcellation into 2514 ROIs in order to get a partition of the entire brain.

UCLA cohort. The study was approved by the IRB Committees of the Veterans Administration as well as of the University of California of Los Angeles (UCLA). After signed informed consent, a group of 15 (7 males) participants between the ages of 30 and 60 was instructed to relax in the resting state avoiding falling asleep. A total of 244 frames were acquired with a TR = 2.500 ms, TE = 30 ms and a flip angle = 80°. The pre-processing of the data was similar to the Bilbao dataset except that it was re-sampled to a $4 \times 4 \times 4$ mm resolution.

Results. – We start by characterizing some elementary statistical features. First, we determine whether the skewness value has any clear spatial distribution across brain structures by analyzing this quantity on each of the 90 Brodmann areas. In each region we compute the average BOLD signal and determine the skewness value (fig. 1). For the same Brodmann area situated in different hemispheres, the skewness value does not differ significantly, as expected since it is known that the BOLD time series of homologous areas are correlated. In addition, this analysis shows that cortical regions exhibit mainly skew positive values, whereas subcortical areas exhibit negative values, as depicted in fig. 1.

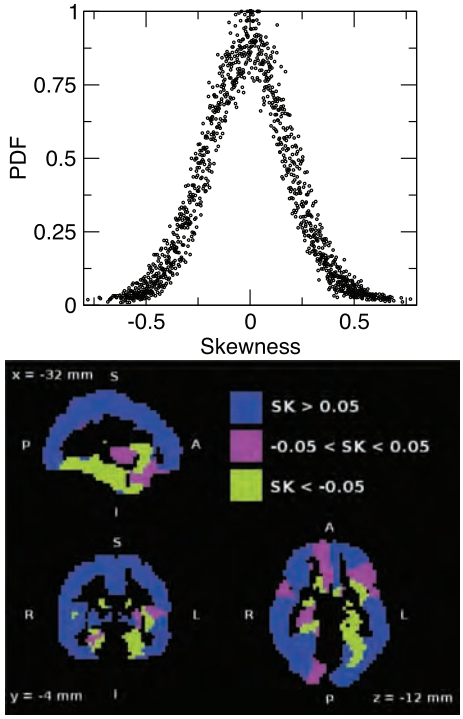

Fig. 1: (Color online) Distribution of brain BOLD signal skewness. The top panel illustrates the (normalized) skewness density distribution of the BOLD signal recorded at the gray matter's voxels of six healthy subjects. The bottom panel shows that the BOLD signals from cortical and subcortical areas exhibit different skewness values (sk). After parcellation of the data in 90 Brodmann areas, the skewness of the average BOLD signal in each area was computed, and then averaged across six healthy subjects. Areas with BOLD signals exhibiting $sk > 0.05$ are indicated in blue, in green areas with $sk < -0.05$ and in pink areas with intermediate values. The activity of cortical areas exhibits positive values, whereas negative skewness values are found in subcortical zones.

Related to this topic, are the recent results by Davis *et al.* [28] proposing an *ad hoc* quantity to characterize the asymmetry of the BOLD signals. The authors defined the *Amplitude Variance Asymmetry* (*AVA*) metric as the ratio between the variance of local maxima and the variance of local minima in a BOLD time course (see fig. 2). For symmetrical BOLD signals the variance of local maxima is similar to the variance of local minima resulting in an AVA value of one. The authors defined two regimes: a "*ceiling mode*", where the variance of local maxima is larger than the one of local minima (AVA > 1), and a "*floor mode*" where the variance of local-minima is larger than the one of local maxima (AVA < 1).

A careful inspection of the BOLD signal should suggest that the skewness of the time series might be related to Davis *et al.*'s asymmetry. By evaluating the third moment in the amplitude distribution, we can determine whether a sequence is symmetric with respect to its mean. For a sequence x_i of length n, the skewness is given by

$$sk = \frac{\frac{1}{n}\sum_{i=1}^{n}(x_i - \bar{x})^3}{\left(\sqrt{\frac{1}{n}\sum_{i=1}^{n}(x_i - \bar{x})^2}\right)^3}, \qquad (1)$$

where $\bar{x}$ is the mean value of the sequence.

Qualitatively, null skewness indicates a symmetric distribution, while a negative/positive skewness value is related to a longer tail on the left/right side of the density probability function, whereas most values (including the median) are situated to the right/left of the mean. While both skewness and the AVA values quantify the same asymmetry in BOLD time series, skewness is nonparametric.

As expected a functional relation between the skewness and the AVA value is demostrated (fig. 2(A)), by computing both quantities for each voxel in the entire brain. We used the logarithmic value of AVA in order to have positive and negative ranges of values, such as the ones for the skewness. Comparing both indicators we can notice that the "ceiling mode" and the "floor mode" reported by Davis *et al.* correspond to the presence of extreme events (up to ~ 8 (fig. 2(E))) in the BOLD time series, that skew the amplitude distribution, resulting in a skewness value different from zero. It will be shown that Davis *et al.*'s

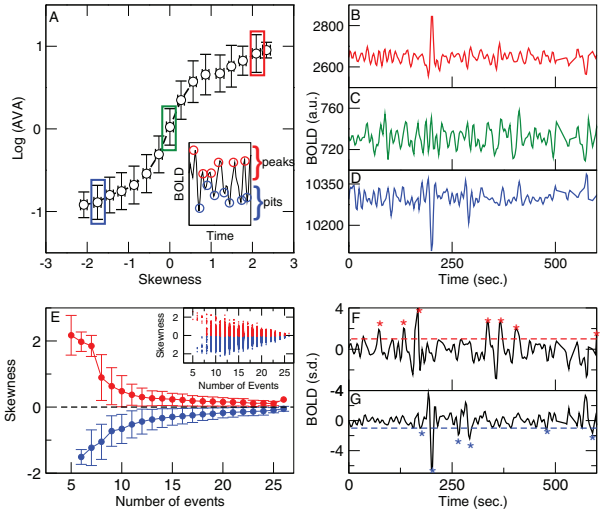

Fig. 2: (Color online) The skewness and the AVA index are equivalent estimations of the BOLD signal higher-order statistics. Panel (A) shows AVA as a function of the skewness value averaged over all brain voxels in one subject. The inset illustrates the two sets (peaks and pits) from which the AVA index is defined. Panels (B) through (D) depict three examples of BOLD signals corresponding to the colored boxes in panel (A). Typically, nonzero values of skewness relate to the existence of one or more extremely large (negative or positive) amplitude events. Panel (E) shows how skewness behaves as a function of the number of extreme events for all voxels in one brain. Inset: we separated the skewness values into two groups: positive skewness (red) and negative skewness (blue), and count the number of peaks (events) above 1 s.d. (dashed lines and asterisks as depicted in the examples presented in (F) and (G)). The averaging over the number of extreme events demonstrates that significant skewness (different from 0) values are found for BOLD signals with up to ~ 8 extreme events.

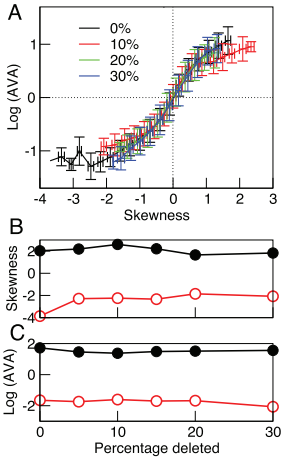

Fig. 3: (Color online) The estimation of skewness and AVA are both inmune to potential head motion's artifacts. (A) Logarithm of AVA as a function of skewness for the raw time series (black), and for different degrees of corrections corresponding to deleting 10 (red), 20 (green) and 30% (blue) of frames, potentially contaminated with head motion. (B) and (C): the range of maximum and minimum values for both AVA and skewness remains approximately constant despite the different degree of motion corrections.

definition can be mapped to the usual higher-moments statistics.

Testing for spurious artifacts. Despite the efforts to mechanically restrain the subject head during the recording, it is known that brief and transient small movements still occur. Thus, it is important to control for the possibility that the presence of extreme events in the BOLD signals is due to spurious motion artifacts. Therefore, we accounted for this possibility by first correcting movements in the pre-processing of the data using the MCFLIRT [29] tool of the *FSL* software. From this first step we saved the time series of residuals, corresponding to the motion along the six degrees of freedom: translation $(x(t), y(t), z(t))$ and rotation $(Rx(t), Ry(t), Rz(t))$. Since the largest source of error comes from translations, we limited our analysis to these degrees of freedom. The absolute translation time series, defined as $T(t) = (x(t)^2 + y(t)^2 + z(t)^2)^{1/2}$, and a threshold U were used to identify the instances with $T(t)$ values above this threshold. Those times $t(i)$ correspond to relatively large motion, thus we tested for their contribution to extreme events in the following manner: the value of the BOLD signal at $t(i)$, in the entire brain, was replaced by the value resulting from performing a linear interpolation between the BOLD signal at times $t(i-1)$ and $t(i+1)$. This was repeated for a range of U values resulting in a deletion of up to 30% of the original BOLD time series.

As shown in fig. 3(A) the functional shape of the relation between the skewness and the AVA values remains unchanged despite a sensible reduction in the datasets. Moreover, the range of skewness values is also independent of the percentage of volumes analyzed once this becomes larger than 10% (fig. 3(B)). From this analysis we conclude that extreme events, and consequently the BOLD time series statistics, are not originated from spurious head motion artifacts and that similar values of skewness are preserved from the original time series to very short ones, achieved after removal of up to 30% of the original time points.

Combined analysis of dynamics and structure. Next we turn to analyzing the relation between the higher-order statistics and the underlying structure. Since the BOLD signal can be shaped by the structural features of the brain network, we analyze the relation between the structural topology of a node and the skewness of the signal at the node. We perform a combined analysis of the BOLD signal at each volume with the level of connectivity of the underlying structural network.

For that purpose, we apply a statistical analysis originally developed to evidence magnitude correlations in seismic catalogs [30] and already used to demonstrate the presence of correlations among extreme events in brain

activity [21]. This approach is based on a systematic comparison between conditional probabilities evaluated in the raw time series and conditional probabilities evaluated in a time series where the activity is randomly reshuffled. In this way one explicitly takes into account the role of statistical fluctuations, which can obscure significant correlations in experimental time series. For each subject, we start by evaluating at each ROI the skewness sk of the time series and the total number of fibers k as the sum of all fibers connecting that ROI to any other ROI in the system.

We then evaluate the conditional probability to measure a skewness with value larger than sk_0 in all ROIs with connectivity larger than k_0, $P(sk > sk_0|k > k_0)$, where sk_0 and k_0 are fixed values of the skewness and connectivity degree chosen in their distributions. For each pair of parameters, we also evaluate the probability $P^*(sk > sk_0|k > k_0)$ for several independent random realizations of a catalog where the skewness values at ROIs are randomly reshuffled, but keeping their connectivity degree. For 10^5 independent realizations of reshuffled data, we find that P^* is distributed as a Gaussian with mean value $Q(sk_0, k_0)$ and standard deviation $\sigma(sk_0, k_0)$, since data are uncorrelated by construction.

The relevant quantity for our analysis is then $\delta P(sk > sk_0, k > k_0) = P(sk > sk_0|k > k_0) - Q(sk_0, k_0)$, *i.e.* the difference between the value of P in the real catalog and its mean value in reshuffled catalogs. If $\delta P(sk > sk_0, k > k_0) > \sigma(sk_0, k_0)$, we can say that the number of ROIs satisfying both conditions, $sk > sk_0$ and $k > k_0$, is larger in the real time series than in any realization of reshuffled catalogs and, therefore, we conclude that activity and connectivity are positively correlated. Conversely, if $|\delta P(sk > sk_0, k > k_0)| < \sigma(sk_0, k_0)$, the value measured in the real temporal series is compatible with values obtained for reshuffled catalogs and, therefore, quantities are uncorrelated.

In fig. 4 (top) we show the value of $\delta P(k > k_0, sk > sk_0)$ evaluated for all ROIs in the system and averaged for the 12 subjects as a function of sk_0 and for different values of k_0. For each value of δP we draw the error bar equal to $\sigma(sk_0, k_0)$ and inspect if the error bar excludes the value $\delta P = 0$. In this case there is evidence for the existence of correlations. Data show that for small values of k_0 the local activity on average does not exhibit relevant correlations with the ROI connectivity. However, for $k_0 \geq 50$ a clear maximum is detected for values of the skewness in the range $(-0.3, -0.2)$, whose positive value excludes $\delta P = 0$, considering error bars. We conclude that there is evidence of correlations for ROIs with skewness $-0.3 < sk < -0.2$. Since $\delta P(sk > sk_0, k > k_0)$ decays to zero for $sk > -0.2$, we conclude that highly connected regions ($k > 50$) tend to exhibit a high activity level as evidenced by a large negative skewness. This result is confirmed if we use $2\sigma(sk_0, k_0)$ as error bar. A similar conclusion can be drawn from fig. 4 (bottom), where $\delta P(sk > sk_0, k > k_0)$ is plotted as function of k_0 for different sk_0. The two curves

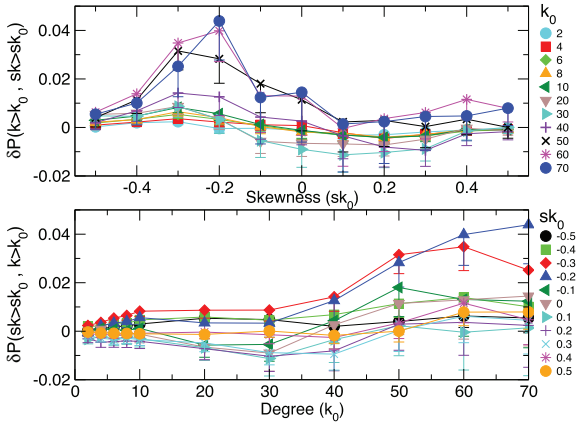

Fig. 4: (Color online) Correlations between the higher-order statistics of the brain activity at one point and its local underlying connectivity. Top: conditional probability difference $\delta P(k > k_0, sk > sk_0)$ as a function of the connectivity parameter k_0 for different skewness parameter sk_0. Bottom: conditional probability difference $\delta P(sk > sk_0, k > k_0)$ as a function of sk_0 and for different values of k_0. Error bars are equal to $\sigma(sk_0, k_0)$.

obtained for $k_0 = -0.2$ and -0.3 show an evident increase as a function of k_0 with respect to the other curves, with the error bar excluding $\delta P = 0$. Finally we notice that there is not a clear evidence of correlations between ROIs with positive skewness and connectivity, and only for $k_0 = 60$ the conditional probability exhibits a relatively small smooth maximum for $sk_0 = 0.4$ (fig. 4, top). This suggests that correlations play a relevant role in regions with high negative skewness, *i.e.* activity is strongly correlated to local connectivity in subcortical areas, and that the relation between activity and connectivity is nonlinear.

Discussion and conclusion. – In this work we have studied the third-moment statistics of the brain BOLD signal in the resting state and its relation with the underlying structural connectivity. We find that the BOLD signal exhibits typically nonzero skewness, with positive values for cortical regions and negative values for subcortical regions. Furthermore, the combined analysis of structural and functional connectivity shows that the amplitude of the signal's skewness at a given region is directly related with the structural degree of the region.

The present results parallel the findings by Davis *et al.* [28] using an *ad hoc* asymmetry index. The fact that the BOLD signal skewness can be equivalent to Davis *et al.*'s index [28], suggests some discussion of their conclusions in the light of the structural-functional relation presented here. The authors in [28] concluded that the main difference in the resting activity profiles of asymmetry were found between adults and children. Furthermore, and perhaps being the most intriguing result, these differences were related with the fact that children with higher IQ exhibited adult-like AVA patterns. Although we did not investigate this issue in our study, the structural

underlying patterns we found seem to support the previous results, since developmental changes are usually related with structural changes.

Interestingly, our results show that negative skewness correlates with more connected regions. In recent work it has been shown that developing hippocampal networks follow a scale-free topology with the existence of functional hubs. In addition, these functional hubs are composed by a subpopulation of GABAergic inhibitory intraneurons [31]. The fact that inhibitory neurons work as hubs may give insights into the observed correlations between negative skewness values and high connectivity. Negative skewness values represent transient extreme events of the BOLD signal below the mean signal value, and may arise from collective cooperation of fast de-activation processes. The fact that inhibitory neurons are organized as functional hubs, may explain why correlations are found between highly connected areas and negative skewness values.

The finding that skewness varies across cortical and subcortical regions suggests future work to elucidate how skewness and structural connectivity relate to the topographical brain distribution. Overall, the present results indicate that higher-order statistics and its structural relation reflect important and novel dimensions of brain dynamics that deserve further exploration.

* * *

Work supported by CONICET (Argentina) (DRC); by Ikerbasque, Euskampus at UPV/EHU, Gobierno Vasco (Saiotek SAIO13-PE13BF001) (JMC) and Ikerbasque Visiting Professor and Bizkaia Talent (AYD-000-285) (SS). Thanks go to I. Escudero and B. Mateos for help in scanning and to the Institute for Theoretical and Computational Physics at University of Granada for the use of computing facilities.

REFERENCES

[1] Eguiluz V. M. *et al.*, *Phys. Rev. Lett.*, **94** (2005) 018102.
[2] Sporns O., Chialvo D. R., Kaiser M. and Hilgetag C. C., *Trends Cogn. Sci.*, **8** (2004) 418.
[3] Craddock R. C. *et al.*, *Nat. Methods*, **10** (2013) 524.
[4] Park H. J. and Friston K., *Science*, **342** (2013) 1238411.
[5] Zhou C. *et al.*, *Phys. Rev. Lett.*, **97** (2006) 238103.
[6] Damoiseaux J. S. and Greicius M. D., *Brain Struct. Funct.*, **213** (2009) 525.
[7] Wang Z. *et al.*, *Neuroscientist*, **21** (2015) 290.
[8] Hagmann P. *et al.*, *PLoS Biol.*, **6** (2008) e159.
[9] Honey C. J. *et al.*, *Proc. Natl. Acad. Sci. U.S.A.*, **106** (2009) 2035-2040.
[10] Fraiman F., Balenzuela P., Foss J. and Chialvo D. R., *Phys. Rev. E*, **79** (2009) 061922.
[11] Haimovici A., Tagliazucchi E., Balenzuela P. and Chialvo D. R., *Phys. Rev. Lett.*, **110** (2013) 178101.
[12] Moretti P. and Muñoz M. A., *Nat. Commun.*, **4** (2013) 2521.
[13] Marinazzo D. *et al.*, *PLoS ONE*, **9** (2014) 1e93616.
[14] Goñi J. *et al.*, *Proc. Natl. Acad. Sci. U.S.A.*, **111** (2014) 833.
[15] Kolchinsky A. *et al.*, *Front. Neuroinform.*, **8** (2014) 66.
[16] Diez I. *et al.*, *Sci. Rep.*, **5** (2015) 10532, arXiv:1410.7959.
[17] Tagliazucchi E., Balenzuela P., Fraiman D. and Chialvo D. R., *Front. Physiol.*, **3** (2012) 15.
[18] Tagliazucchi E. *et al.*, *Neurosci. Lett.*, **488** (2011) 158.
[19] Petridou N. *et al.*, *Hum. Brain Mapp.*, **34** (2013) 1319.
[20] Liu X. and Duyn J. H., *Proc. Natl. Acad. Sci. U.S.A.*, **110** (2013) 4392.
[21] Lombardi F., Chialvo D. R., Herrmann H. J. and de Arcangelis L., *Chaos, Solitons Fractals*, **55** (2013) 102.
[22] Mori S., Crain B. J., Chacko V. P. and van Zijl P. C., *Ann. Neurol.*, **45** (1999) 265.
[23] Wang R., Benner T., Sorensen A. G. and Wedeen V. J., *Proc. Int. Soc. Magn. Reson. Med.*, **15** (2007) 3720.
[24] Mori S. and van Zijl P. C., *NMR Biomed.*, **15** (2002) 468.
[25] Jezzard P., Mathews P. and Smith S. M., *Functional MRI: An Introduction to Methods* (Oxford University Press, Oxford) 2001.
[26] Cordes D. *et al.*, *Am. J. Neuroradiol.*, **22** (2001) 1326.
[27] Craddock R. C. *et al.*, *Hum. Brain Mapp.*, **33** (2012) 1914.
[28] Davis B., Jovicich J., Iacovella V. and Hasson U., *Cereb. Cortex*, **24** (2014) 1332.
[29] Jenkinson M., Bannister P., Brady M. and Smith S., *Neuroimage*, **17** (2002) 825.
[30] Lippiello E., de Arcangelis L. and Godano C., *Phys. Rev. Lett.*, **100** (2008) 038501.
[31] Bonifazi P. *et al.*, *Science*, **326** (2009) 1419.